

# 112 Gb/s Sub-Cycle 16-QAM Nyquist-SCM for Intra-Datacenter Connectivity

Paraskevas Bakopoulos<sup>\*a</sup>, Stefanos Dris<sup>a</sup>, Nikolaos Argyris<sup>a</sup>, Christos Spatharakis<sup>a</sup>, Hercules Avramopoulos<sup>a</sup>

<sup>a</sup>Photonics Communications Research Laboratory, National Technical University of Athens, Iroon Polytechniou 9, Zografou GR-15780, Greece

## ABSTRACT

Datacenter traffic is exploding. Ongoing advancements in network infrastructure that ride on Moore's law are unable to keep up, necessitating the introduction of multiplexing and advanced modulation formats for optical interconnects in order to overcome bandwidth limitations, and scale lane speeds with energy- and cost-efficiency to 100 Gb/s and beyond. While the jury is still out as to how this will be achieved, schemes relying on intensity modulation with direct detection (IM/DD) are regarded as particularly attractive, due to their inherent implementation simplicity. Moreover, the scaling-out of datacenters calls for longer transmission reach exceeding 300 m, requiring single-mode solutions.

In this work we advocate using 16-QAM sub-cycle Nyquist-SCM as a simpler alternative to discrete multitone (DMT), but which is still more bandwidth-efficient than PAM-4. The proposed optical interconnect is demonstrated at 112 Gb/s, which, to the best of our knowledge, is the highest rate achieved in a single-polarization implementation of SCM. Off-the-shelf components are used: A DFB laser, a 24.3 GHz electro-absorption modulator (EAM) and a limiting photoreceiver, combined with equalization through digital signal processing (DSP) at the receiver. The EAM is driven by a low-swing (<1 V) arbitrary waveform generator (AWG), which produces a 28 Gbaud 16-QAM electrical signal with carrier frequency at ~15 GHz. Tight spectral shaping is leveraged as a means of maintaining signal fidelity when using low-bandwidth electro-optic components; matched root-raised-cosine transmit and receive filters with 0.1 excess bandwidth are thus employed. Performance is assessed through transmission experiments over 1250 m and 2000 m of SMF.

**Keywords:** Optical Interconnects, sub-carrier modulation, 16-QAM, Nyquist pulse shaping, intra-datacenter connectivity, direct detection, digital equalization.

## 1. INTRODUCTION

Datacenter traffic is skyrocketing, fueled by ubiquitous high-definition video and the rapid uptake of cloud applications and machine-to-machine (M2M) communication. Sustained annual growth rates as high as 25% are expected until the end of the decade, with the largest part of this enormous traffic residing inside the datacenter as a result of server virtualization and resource disaggregation. This soaring need for capacity is overwhelming optical interconnects for intra- or short inter-datacenter links, also known as client optics. Industry roadmaps herald that systems with aggregate capacity of 400 Gb/s will need to be deployed in the early 2020s<sup>1</sup>. A viable solution for early deployments based on currently available optoelectronics would be to increase the number of channels e.g. using 16 WDM or parallel fiber ribbon lanes, however this approach comes with sublime challenges for reducing module size and power consumption<sup>2</sup>. Scaling per-channel speed to 100 Gb/s is therefore deemed essential for the deployment of efficient 400 Gb/s systems<sup>3</sup>. The feasibility of serial 100 Gb/s connectivity using non-return-to-zero (NRZ) modulation has been demonstrated in<sup>4</sup> based on specialized state-of-the-art photonics and electronics technologies, but, in order to reach the cost and energy consumption targets for future systems, implementation with available CMOS nodes is an outright requirement. With CMOS speeds unable to keep pace with surging interconnect lane speeds, there is growing consensus among academia and industry towards migration to higher-order modulation (HOM) providing more bits-per-symbol<sup>3,5</sup>.

Unlike ongoing progresses in optical transport networks where HOM is achieved with complex modulation of the optical field and coherent detection at the receiver, the extremely cost-sensitive datacenter environment designates the use of simple intensity modulation with direct detection (IM/DD). Quaternary Pulse-amplitude modulation (PAM-4) is gaining traction for 56 Gb/s per lane such as CEI-56G-VSR-PAM-4 and IEEE P802.3bs due to its compatibility with 28 Gb/s

---

<sup>\*</sup>[pbakop@mail.ntua.gr](mailto:pbakop@mail.ntua.gr), <http://photonics.ntua.gr>

optics and simple generation of the driving signal, that can avoid the use of a sophisticated digital-to-analogue converter (DAC)<sup>6,7</sup>. Further scaling bandwidth efficiency to 4 bits/symbol with higher-order PAM in order to reach 100 Gb/s poses a number of practical limitations due to the stringent SNR requirements that stem from the non-optimal constellation of PAM systems. As an alternative for achieving 100 Gb/s on a single optical carrier using 28 Gb/s optoelectronics, discrete multi-tone modulation (DMT) has been proposed. DMT is ubiquitous in digital subscriber loop (DSL) copper links and defines the optimum bitrate adaptively for each subcarrier based on the SNR. Its application in optical links vouches for optimal use of the available channel even in the presence of impairments like notches in the electro-optic response of the transmitter and receiver PCB. Generation of 100 Gb/s on a single optical carrier using DMT and transmission over 2 km of single-mode fiber (SMF) was demonstrated in<sup>8</sup>. Comparison with 100 Gb/s PAM-M (M=4, 8 and 16) revealed the superior BER performance of DMT and its higher resilience to bandwidth limitations. On the downside, DMT introduces added complexity due to the fast Fourier transform operations required at the transmitter and receiver side and the use of adaptive bit-loading algorithms that require feedback from the receiver to the transmitter. In addition, DMT inherently suffers from poor power efficiency owing to its high peak-to-average power ratio (PAPR) and is sensitive to DFB nonlinearities and RIN.

An alternative approach to mitigate these shortcomings is subcarrier modulation (SCM), where a QAM signal is modulated onto an electrical RF subcarrier before driving an intensity modulator or a directly-modulated laser. Sub-carrier 16-QAM modulation with Nyquist pulse shaping has been shown to outperform DMT considering equivalent systems at 100 Gb/s by virtue of its lower PAPR, better tolerance to DFB nonlinearity and higher resilience to laser relative intensity noise (RIN)<sup>2,9</sup>. Transmission of a 56 Gb/s sub-cycle 16-QAM signal over 4 km of single-mode fiber in the C-band was demonstrated in<sup>10</sup> using a directly-modulated passive feedback laser (PFL). Extension to 112 Gb/s was achieved by means of polarization multiplexing, which however doubles the component count at the transmitter and receiver sides and necessitates real-time compensation of polarization drifts at the receiver. A single-wavelength, single polarization 112 Gb/s sub-cycle 16-QAM system was very recently demonstrated in<sup>11</sup>. The system relied on a 25 Gb/s externally-modulated laser (EML) and obtained transmission over 10 km of single-mode fiber in the low-dispersion O-band.

Generation of the half-cycle QAM signal can be performed in the analog<sup>12</sup> or digital domain<sup>9-11</sup>, with the latter approach offering additional design flexibility. A digital implementation offers extensive equalization capabilities in contrast to analogue equalizers that only work well in fairly flat channels. Even more, the digital approach allows for custom, non-rectangular constellations that can further improve system performance<sup>13</sup>. The feasibility of a fully-digital implementation of 100 Gb/s half-cycle QAM is underpinned by the availability of commercial CMOS DAC and ADC cores operating at 65 GSa/s<sup>14</sup>. Capitalizing on the energy efficiency of advanced CMOS nodes, these data converters dissipate approximately 1 W per channel<sup>15,16</sup> and are therefore compatible with the requirements of client optics. An implicit pitfall of this approach is the discrepancy between the low-voltage capability of CMOS DACs and the driving requirements of typical EMLs and DMLs (e.g. 4 V<sub>pp</sub> in<sup>10</sup>, 1.7 V<sub>pp</sub> in<sup>11</sup>) which entails the use of a linear driver amplifier, increasing power consumption and bill of materials, while hindering close integration of the CMOS ASIC with the optics. Avoiding the use of a driver amplifier is therefore pivotal for the viability of this approach in 100 Gb/s interconnects with small form factor.

In this paper we demonstrate for the first time a single-polarization 112 Gb/s digital 16-QAM optical link operating in the C-band. This spectral region is attracting particular interest for client optics applications<sup>17</sup> despite the more pronounced effects of chromatic dispersion, due to the vast availability of photonic components. Transmission over 2 km of single-mode fiber is demonstrated assuming a simple hard-decision FEC with 10% overhead, which is commonplace for single-wavelength 100 Gb/s interconnects. A commercial electro-absorption modulator is driven directly by the CMOS data converter at sub-volt electrical swing, demonstrating the feasibility of eliminating the need for costly and inefficient linear driver amplifier. The performance of the system is compared to an equivalent implementation with PAM-8 modulation showing superior performance.

## 2. CONCEPT

Subcarrier modulation relies on the modulation of a QAM signal on an electrical RF subcarrier, which is further intensity-modulated on the optical carrier. The frequency of the RF subcarrier,  $f_{sc}$ , is a crucial parameter of the system; it needs to remain as low as possible in order to reduce the excess electro-optical bandwidth required to accommodate the SCM signal. To avoid aliasing,  $f_{sc}$  can be set equal to the symbol rate  $f_{sym}$ , thus requiring an overall optical bandwidth of twice the symbol rate (Figure 1(d)). This approach is often referred to as single-cycle SCM and was validated in<sup>18</sup> with the generation of a 56 Gb/s 16-QAM signal in a Mach-Zehnder modulator using a 14 GHz RF subcarrier. To further reduce the required bandwidth of the SCM signal it is possible to apply filtering to the baseband I and Q components before up-conversion to

$f_{sc}$ . Nyquist filtering can ideally restrict the bandwidth of the baseband signal to  $f_{sym}/2$ , thus it is possible to accommodate the SCM signal without aliasing even when the subcarrier frequency is set to exactly half the symbol rate, in a configuration referred to as half-cycle SCM (Figure 1(e) and respective baseband signal in Figure 1(b)). In practice, generation of an ideal Nyquist-shaped signal raises significant challenges as it entails the implementation of a digital raised-cosine filter with a roll-off factor  $\alpha = 0$ . A reduction in implementation complexity can be achieved by relaxing the roll-off factor, so as to strike a better balance between excess bandwidth and number of filter taps. In this approach, which falls within the general category of sub-cycle SCM, the RF subcarrier is slightly above the ideal  $f_{sym}/2$  of half-cycle SCM, thus accommodating the up-conversion of a Nyquist-shaped QAM signal with non-zero roll-off factor yet without consuming too much excess bandwidth (Figure 1(f) and (c)).

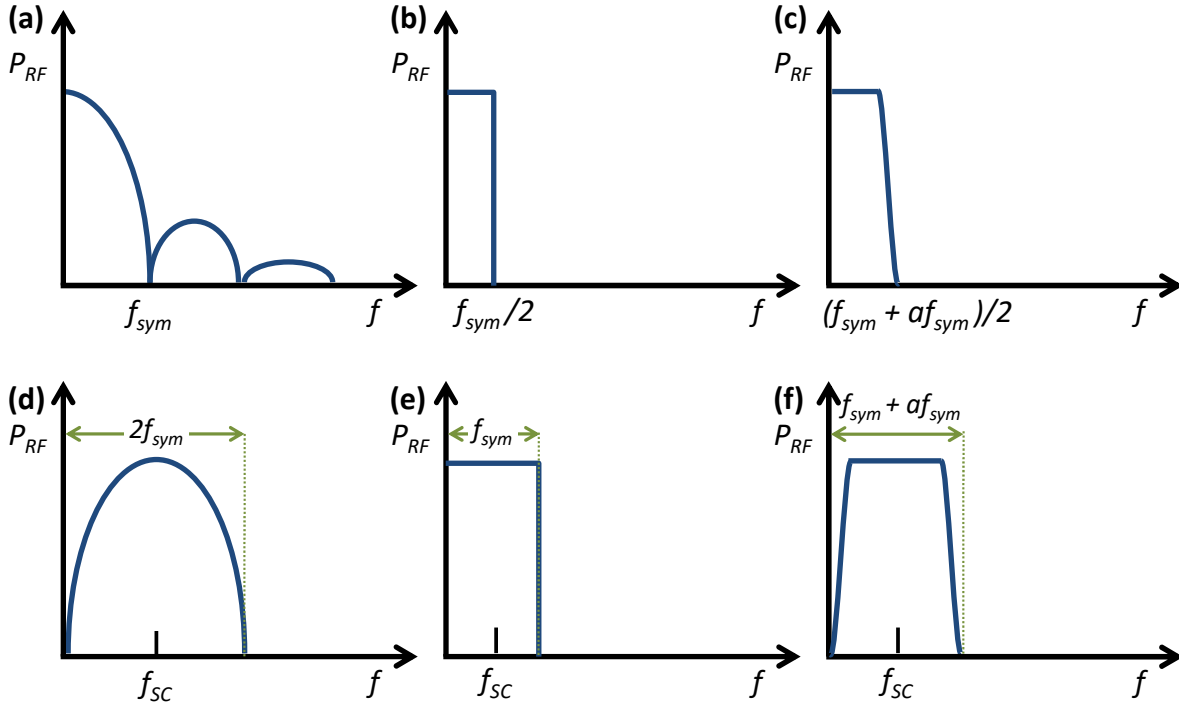


Figure 1. Indicative spectra of (a) NRZ baseband signal, (b) ideal Nyquist baseband signal, (c) Nyquist baseband signal with non-ideal roll-off factor  $\alpha$ , (d) single-cycle NRZ-SCM (side-lobes higher than  $f_{sym}$  are assumed to be filtered out to avoid aliasing), (e) half-cycle Nyquist SCM and (d) sub-cycle Nyquist SCM with roll-off factor  $\alpha$ .

### 3. SCM AND PAM-8 SIMULATIONS

The first step in order to explore and validate the efficiency of the SCM concept was to simulate an optical interconnect link employing IM/DD in VPItransmissionMaker™. As a reference for comparison, a 40 Gbaud PAM-8 signal was selected, since the resulting bitrate of 120 Gb/s is very close to that of our SCM scheme (112 Gb/s). For both signals pulse-shaping was employed so as to limit the effects of a bandlimited channel as much as possible. The 3 dB bandwidth of the optical channel was chosen to be 40 GHz.

#### 3.1 Methodology and simulation setup

The setup used for simulating the 40 GHz optical interconnect link is shown in Figure 2. Both SCM and PAM-8 signals were generated and processed (Tx-side DSP) in MATLAB using a repeating random input stream with pattern length of  $2^{15}$  symbols. For the SCM case, the baseband electrical 16-QAM signal was modulated using a QAM mapper and filtered through a Root-Raised-Cosine Filter with roll-off factor  $\alpha = 0.1$ . The pulse-shaped signal was up-converted to a 15.4 GHz carrier signal as shown in Figure 3. The amplitude of the signal was normalized to  $1 V_{pk-pk}$  to emulate the limited electrical swing typical of CMOS DAC cores, in consistency with the experiment. The generated electrical SCM signal was finally imported to VPItransmissionMaker™. In the case of PAM-8 the signal generation was similar, except for the up-conversion function that was bypassed and the symbol mapper that was adjusted to PAM-8 for this case.

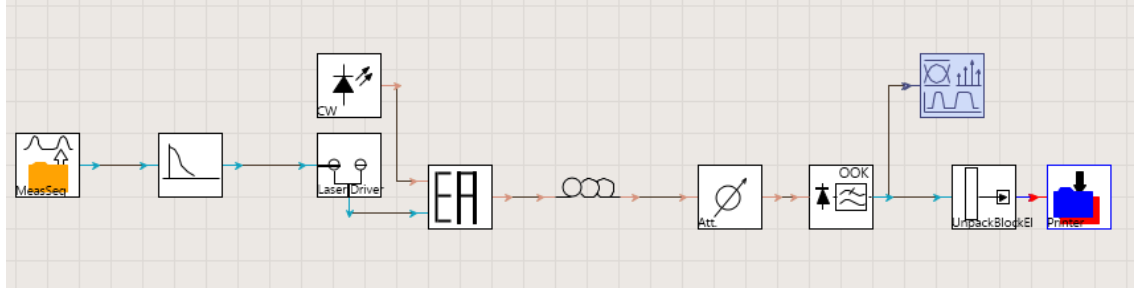


Figure 2. Setup of a 40 GHz optical interconnect in VPItransmissionMaker used for SCM and PAM-8 simulations.

The imported waveform from MATLAB was introduced into an EAM while a continuous wave (CW) laser generating 0 dBm at 1550 nm was used as the light source. To emulate the overall bandwidth limitation of the channel, an 8<sup>th</sup> order Chebyshev Type II analog filter with 40 GHz 3-dB bandwidth was applied to the EAM driving signal. The length of the optical link was varied to 500, 1000 and 2000 m and a variable optical attenuator (VOA) was used to sweep the received optical power and obtain BER plots as a function of Rx power for the different transmission lengths. The simulated time was set to 80  $\mu$ s which corresponded to a number of transmitted symbols equal to 2 800 000 in both cases. Finally, a linear photoreceiver was employed for direct detection and the received signals were digitized and processed in MATLAB.

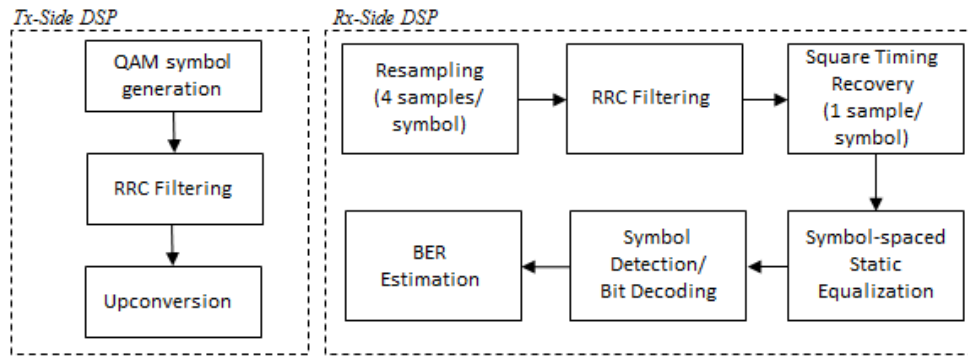


Figure 3. DSP blocks for the transmitter and receiver, implemented in MATLAB.

Figure 3 depicts the DSP blocks employed for the SCM case for the transmitter and receiver. At the receiver side, the signal was resampled using 4 samples per symbol and then filtered through the matched root-raised-cosine Rx filter. Symbol clock recovery using the square timing algorithm was also performed, as well as symbol-spaced linear equalization, thresholding and symbol detection, followed by decoding and BER estimation. As far as the equalizer is concerned, the final static coefficients were obtained by employing a training process of a Feed Forward Equalizer (FFE) operating in decision-directed mode with the normalized least mean squares (LMS) algorithm, at zero receiver attenuation (i.e. at the highest Rx optical power). The number of taps employed was chosen so as to minimize the mean square error (MSE) of the estimation. The number of taps was progressively increased and the coefficients adapted until no significant improvement in MSE could be obtained, and the respective taps were finally selected. The BER for each run was then obtained with the fixed equalizer coefficients determined by the process described.

### 3.2 Simulation results

Figure 4 shows the BER curves obtained via simulation as a function of the received optical power. The solid lines with circular markers correspond to the 28 Gbaud, 112 Gb/s RRC-shaped 16-QAM SCM, while the dotted lines with hollow squares represent the 40 Gbaud, 120 Gb/s RRC-shaped PAM-8. The first observation is that in both cases, there is no penalty associated with increased transmission distance; this can be attributed to the RRC pulse-shaping which confines the spectral content of the signals to a minimum, thereby greatly reducing the effects of chromatic dispersion. Thus, the BER curves for 500, 1000 and 2000 m are almost identical for a given modulation format.

Both SCM and PAM-8 exhibit robust performance for the simulated channel, however the performance of SCM is notably better. The received optical power for which BER  $1 \cdot 10^{-3}$  is achieved is  $\sim 1.4$  dB lower for SCM, compared to the PAM-8 case. It can be concluded that RRC-shaped SCM offers better performance for up to 2 km optical interconnects, when compared to a similar-bitrate RRC-shaped PAM-8 system.

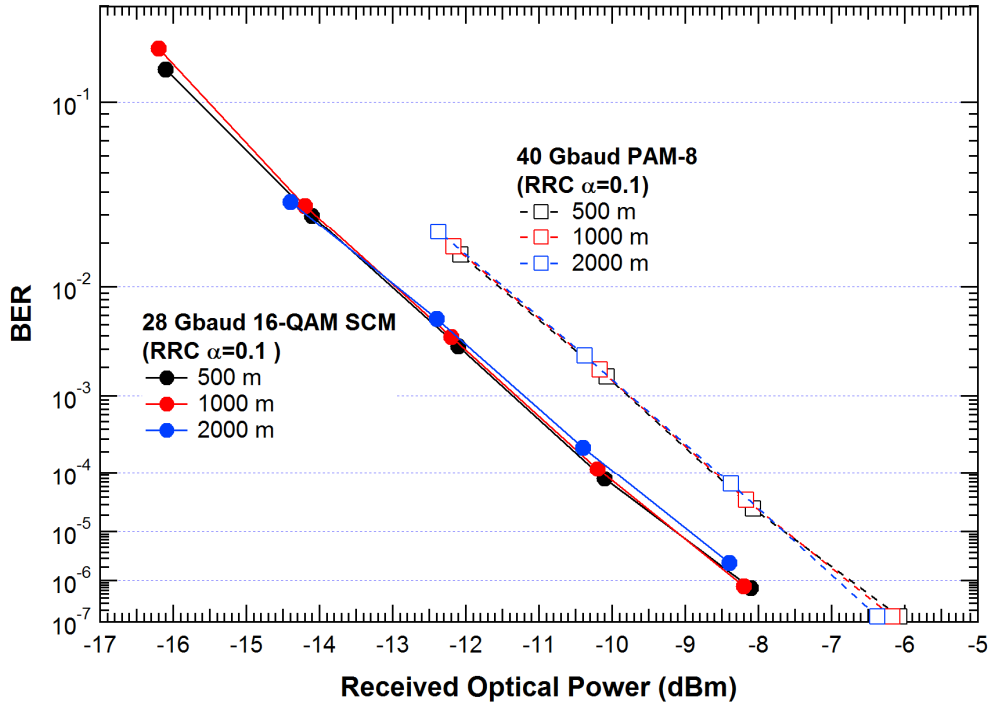


Figure 4. BER curves as a function of the received optical power for 3 different lengths (500,1000 and 2000m) of SMF for the 28 Gbaud 16-QAM SCM signals (solid lines and markers) and the 40 Gbaud PAM-8 signals (dotted lines, hollow markers).

## 4. 16-QAM SCM EXPERIMENT

### 4.1 Experimental setup and DSP

The experimental setup for the generation and reception of the 112 Gb/s sub-cycle SCM is shown in Figure 5. The 112 Gb/s sub-cycle 16-QAM test pattern was provided by the single-ended output of an 8-bit, 65 GSa/s Arbitrary Waveform Generator (AWG), which implemented all the transmitter DSP functions. A repeating pattern of  $2^7$  symbols was generated at 28 Gbaud, using a square 16-QAM constellation mapping. Nyquist filtering was implemented in the digital domain with a roll-off factor  $\alpha=0.1$ , thus restricting the bandwidth of the baseband signal to  $\pm 15.4$  GHz. Digital up-conversion to an RF subcarrier  $f_{sc} = 15.4$  GHz resulted in an SCM signal that was band-limited to 30.8 GHz, which was well beyond the electrical bandwidth of the AWG (20-22 GHz at 3-dB).

The electrical SCM signal from the AWG was introduced to an off-the-shelf electro-absorption modulator, exhibiting a 3 dB electro-optical bandwidth of 24.3 GHz. The voltage swing at the AWG output was 732 mV<sub>pk-pk</sub> and no modulator driver was employed, thus limiting the achievable modulation depth of the EAM to less than 10 dB. The EAM was connected to a DFB laser providing a continuous wave (CW) optical signal at 1560 nm with 7.8 dBm of optical power and 145 dB/Hz relative intensity noise (RIN). The generated multi-level optical signal was transmitted through a 1250 and 2000 m spool of standard SMF. An off-the-shelf 40 Gb/s photoreceiver was used for signal detection, consisting of a waveguide-integrated pin-photodiode (PD) and a transimpedance amplifier (TIA) with limiting output buffer. The photoreceiver exhibited a 3 dB bandwidth of 35 GHz, 0.6 A/W responsivity, 500 V/W conversion gain and -12 dBm sensitivity ( $10^{-12}$  BER,  $2^{31-1}$  PRBS). Due to the limiting operation of the available photoreceiver, operation at low received power was opted to avoid nonlinear distortion. The photoreceiver was connected to a real time oscilloscope with 33 GHz analog bandwidth and 80 GSa/s sampling rate for signal digitization and off-line processing.

As far as the receiver-side DSP is concerned, the offline DSP blocks employed are similar to those described in the previous section. After resampling the digitization to 4 samples/symbol, the signal was fed to the matched RRC Rx filter. The square timing algorithm was then employed for symbol clock recovery, followed by static equalization to compensate for the channel bandwidth limitations. The static FIR coefficients were determined following the same procedure described in the simulation section, by employing an adaptive FFE and using the normalized LMS algorithm to minimize the MSE of a known training pattern. Finally, symbol detection, bit decoding and BER assessment were performed so as to evaluate the optical link's performance.

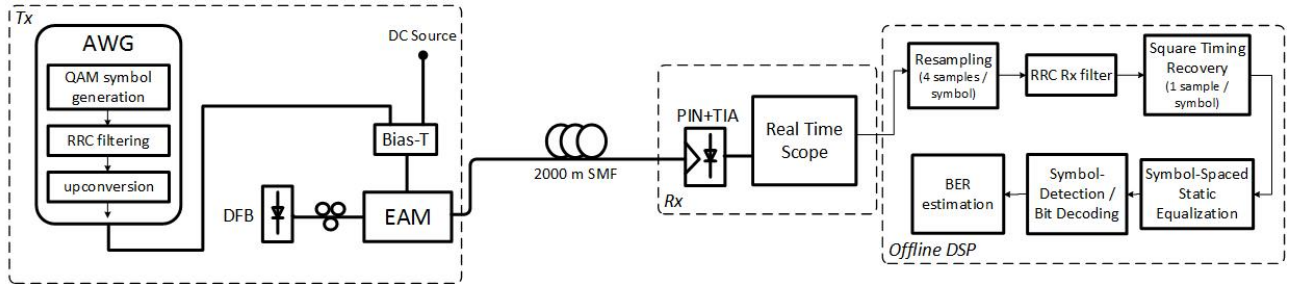


Figure 5. Experimental setup of the 16-QAM Nyquist-SCM optical interconnect and overview of DSP blocks.

## 4.2 Results and discussion

The system's performance was evaluated by means of constellation diagrams of the received signals before and after equalization, as well as BER curves as a function of the received optical power. A comparison is also made with experimental data from a 40 GBaud RRC-shaped PAM-8 transmission experiment, described in<sup>19</sup>. In Figure 6, the back-to-back optical SCM signal is shown at the highest received optical power (-3.9 dBm). On the left side is the received signal without equalization being employed, while on the right side the same signal is shown after static equalization. It is obvious that the bandwidth limitation of the channel severely affects the signal's quality and equalization is necessary to compensate for the channel response. Once equalized, the signal was significantly improved and no errors were observed at that particular received power. Since  $\sim 10^6$  bits were processed, the BER can be estimated to be less than  $\sim 4 \cdot 10^{-7}$  at 95% confidence level. A part of this signal was used as the training sequence for the adaptive FFE in order to determine the weights for the rest of the runs, which were at lower Rx powers. In order to achieve the best possible BER and compensate as much as possible for the signal degradation through the bandlimited and rippled response of the implemented channel, more than 250 taps were employed for all experimental runs.

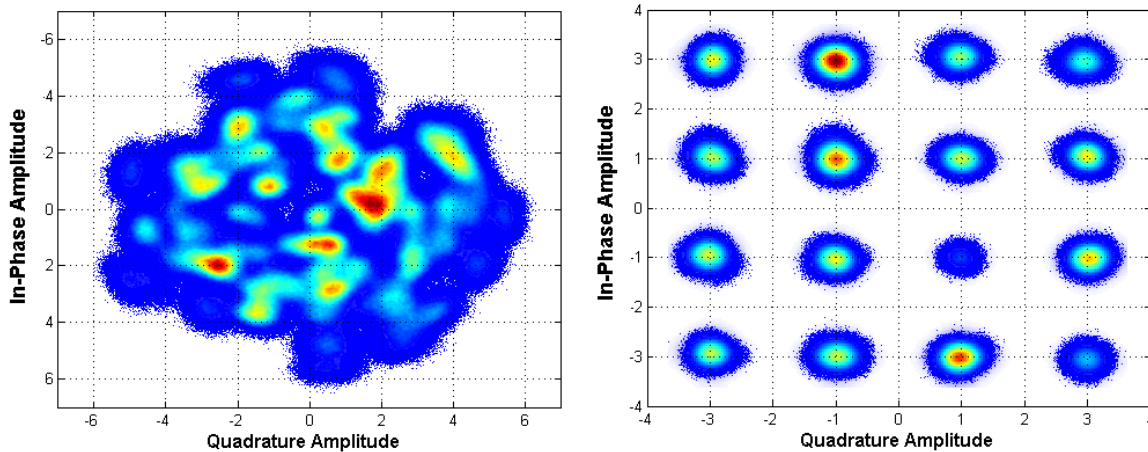


Figure 6. Constellation diagram of the back-to-back optical signal before (left) and after (right) equalization for a received optical power of -3.9 dBm.

Figure 7 and Figure 8 show the constellation diagrams of the highest received power, for transmission over 1250 and 2000 m of SMF respectively. For the 1250 m case, the highest received optical power was measured to be -4.7 dBm and again, since no errors were observed, the BER was estimated at less than  $\sim 4 \cdot 10^{-7}$ . As far as the 2000 m case is concerned, the highest received optical power was -6.8 dBm and the BER was measured at  $2.6 \cdot 10^{-6}$ . These signals were also used to determine the equalizer coefficients for each transmission distance respectively.

From the simulation results of section 3, no quantifiable signal degradation is expected due to chromatic dispersion up to a transmission distance of 2000 m. The BER plots of Figure 9 show only a small penalty between the back-to-back and 2000 m curves, especially at the highest received optical powers.

Compared to the experimental RRC-shaped 40 Gbaud PAM-8 signal (also plotted in Figure 9), the RRC 16-QAM SCM performs better, as predicted by the simulations. The required Rx power at a BER of  $10^{-3}$  for SCM is  $\sim 3.1$  dB better than the PAM-8.

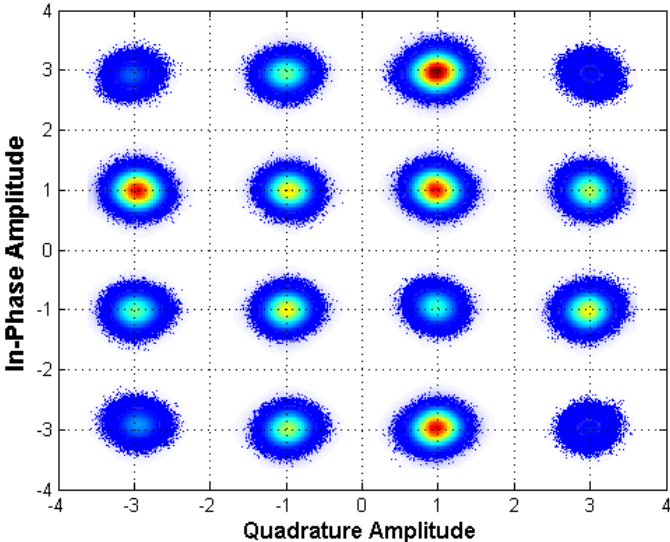


Figure 7. Constellation diagram of the received signal after 1250 m transmission over SMF after equalization for a received optical power of -4.7 dBm.

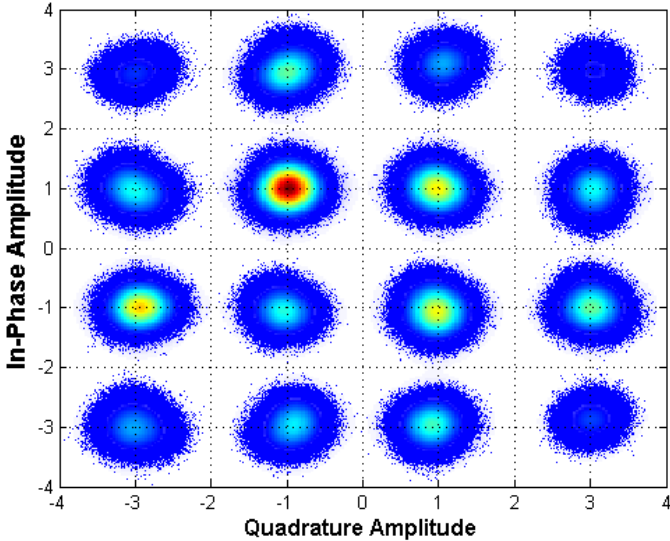


Figure 8. Constellation diagram of the received signal after 2000 m transmission over SMF after equalization for a received optical power of -6.8 dBm.

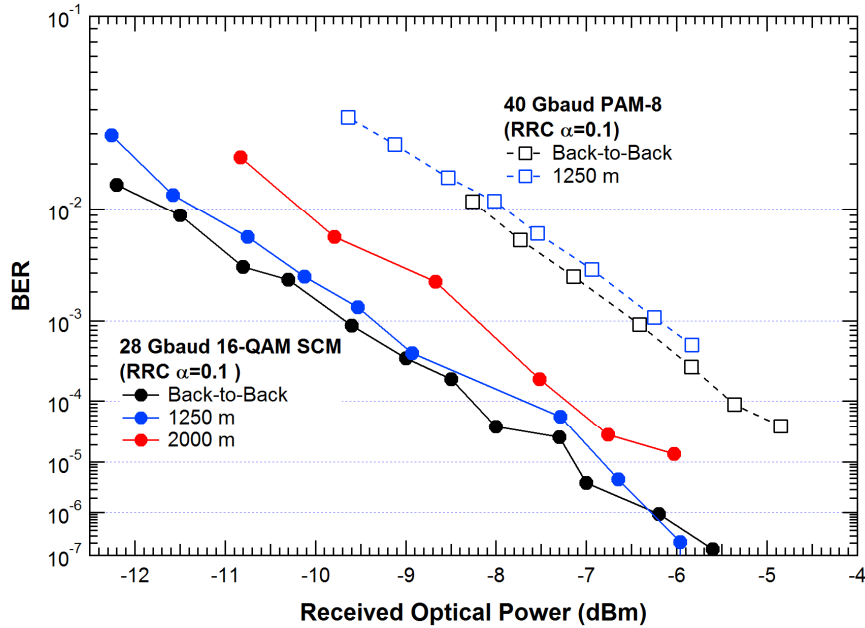


Figure 9. BER curves of the experimental results as a function of the received optical power for back-to-back and transmission (1250 and 2000 m of SMF), for the 28 GBaud 16-QAM SCM signals (solid lines and markers), and back-to-back and transmission (1250 m) for the 40 GBaud PAM-8 signals (dotted lines, hollow markers).

## 5. CONCLUSIONS

We have demonstrated the successful transmission of single-wavelength 112 Gb/s Sub-Cycle 16-QAM Nyquist-SCM over 1250 and 2000 m SMF. QAM signal generation, RRC filtering and frequency up-conversion were carried out in the digital domain at the transmitter. Digital equalization at the receiver side with a linear FFE equalizer compensated the severe bandwidth limitation of the overall channel, achieving operation below the FEC threshold. Comparison with an equivalent 120 Gb/s PAM-8 implementation with identical hardware manifested the superior performance of the 16-QAM Nyquist-SCM system. Direct interconnection of the EAM with the data converter validated the feasibility to operate with sub-volt electrical swing, despite the compromised modulation depth. Hence, the proposed scheme is compatible with state-of-the-art CMOS electronics found in switch or server ICs and is suitable for application in client optics where the driver amplifier represents a significant cost and energy overhead.

## ACKNOWLEDGEMENTS

This work has received funding from the European Union’s Horizon 2020 and FP7 research and innovation programs under grant agreements No 645212 (NEPHELE), No 318240 (PHOXTROT) and 318228 (MIRAGE). The manuscript reflects only the authors’ view and the Commission is not responsible for any use that may be made of the information it contains. The authors gratefully acknowledge Keysight Technologies for providing the AWG.

## REFERENCES

- [1] D’Ambrosia, J. and Kipp, S. G., “The 2015 Ethernet Roadmap”, Ethernet alliance, March 2015, [http://www.ethernetalliance.org/wp-content/uploads/2015/03/EthernetAlliance\\_Roadmap\\_whitepaper\\_FINAL-032015-21.pdf](http://www.ethernetalliance.org/wp-content/uploads/2015/03/EthernetAlliance_Roadmap_whitepaper_FINAL-032015-21.pdf) (18 January 2016).
- [2] Lyubomirsky, I. and Ling, W. A., “Digital QAM Modulation and Equalization for High Performance 400 GbE Data Center Modules,” Proc. OFC, W1F.4 (2014).

- [3] Cole, C., Lyubomirsky, I., Ghiasi A. and Telang, V., "Higher-Order Modulation for Client Optics," IEEE Communications Magazine 51(3), 50-57 (2013).
- [4] Katopodis, V. et. al., "Serial 100 Gb/s connectivity based on polymer photonics and InP-DHBT electronics," Optics Express 20(27), 28538-28543 (2012).
- [5] Apostolopoulos, D. et. al., "Photonic integration enabling new multiplexing concepts in optical board-to-board and rack-to-rack interconnects," Proc. SPIE 8991, Optical Interconnects XIV, 89910D (2014).
- [6] Chen, C, Tang, X. and Zhang, Z., "Transmission of 56-Gb/s PAM-4 over 26-km single mode fiber using maximum likelihood sequence estimation," Proc. OFC, Th4A.5 (2015).
- [7] Soenen, W. et. al., "40 Gb/s PAM-4 Transmitter IC for Long-Wavelength VCSEL Links," IEEE Photonics Technology Letters 27(4), 344-347 (2015).
- [8] Kai, Y. et. al., "Experimental Comparison of Pulse Amplitude Modulation (PAM) and Discrete Multi-tone (DMT) for Short-Reach 400-Gbps Data Communication," Proc. ECOC, Th.1.F.3 (2013).
- [9] Tang, J., He, J., Li, D., Chen, M. and Chan, L., "64/128-QAM Half-Cycle Subcarrier Modulation for Short-Reach Optical Communications," IEEE Photonics Technology Letters 27(3), 284-287 (2015).
- [10] Karar, A. H. and Cartledge, J. C., "Generation and Detection of a 56 Gb/s Signal Using a DML and Half-Cycle 16-QAM Nyquist-SCM," IEEE Photonics Technology Letters 25(8), 757-760 (2013).
- [11] Zhong, K., et. al., "Transmission of 112Gbit/s Single Polarization Half-Cycle 16QAM Nyquist-SCM with 25Gbps EML and Direct Detection," Proc. ECOC, P.4.9 (2015).
- [12] Pham, T. T., Rodes, R., Jensen, J. B., Chang-Hasnain C. J. and Monroy I. T., "Sub-cycle QAM modulation for VCSEL-based optical fiber links," Optics Express 21(2), 1830-1839 (2013).
- [13] Ling, W. A., Lyubomirsky, I. and Solgaard, O., "Digital quadrature amplitude modulation with optimized non-rectangular constellations for 100 Gb/s transmission by a directly-modulated laser," Optics Express 22(9), 10844-10857 (2014).
- [14] Yan, W. Z., et. al., "100 Gb/s optical IM-DD transmission with 10G-class devices enabled by 65 GSamples/s CMOS DAC core," Proc. OFC, OM3H.1 (2013).
- [15] "LEIA digital-to-analog converter," Fujitsu Semiconductor Europe, 29 March 2012, <http://www.fujitsu.com/downloads/MICRO/fme/documentation/c60.pdf> (18 January 2016).
- [16] "LUKE-ES analog-to-digital converter," Fujitsu Semiconductor Europe, 29 March 2012, <http://www.fujitsu.com/downloads/MICRO/fme/documentation/c63.pdf> (18 January 2016).
- [17] OpenOptics MSA, <http://openopticsmsa.org> (18 January 2016).
- [18] Olsson B.-E. and Alping, A., "Electro-optical subcarrier modulation transmitter for 100 GbE DWDM transport," Proc. Opt. Fiber Commun. Optoelectron. Exposit. Conf., SaF3 (2008).
- [19] Dris, S., et al., "Scaling single-wavelength optical interconnects to 180 Gb/s with PAM-M and pulse shaping," Proc. SPIE Photonics West, Paper 9775-4 (2016).